

# Lipid Flip-Flop Driven Mechanical and Morphological Changes in Model Membranes

Sanoop Ramachandran\*

*Department of Physics, Indian Institute of Technology Madras, Chennai - 600 036, India*

P. B. Sunil Kumar†

*Department of Physics, Indian Institute of Technology Madras, Chennai - 600 036, India*

*and MEMPHYS-Center for Biomembrane Physics,*

*University of Southern Denmark, Odense, DK-5230, Denmark*

Mohamed Laradji‡

*Department of Physics, The University of Memphis, Memphis, TN 38152-3390, USA*

*and MEMPHYS-Center for Biomembrane Physics,*

*University of Southern Denmark, Odense, DK-5230, Denmark*

(Dated: May 3, 2019)

## Abstract

We study, using dissipative particle dynamics simulations, the effect of active lipid flip-flop on model fluid bilayer membranes. We consider both cases of symmetric as well as asymmetric flip-flops. Symmetric flip-flop leads to a steady state of the membrane with an effective temperature higher than that of the equilibrium membrane and an effective surface tension lower than that of the equilibrium membrane. Asymmetric flip-flop leads to transient conformational changes of the membrane in the form of bud or blister formation, depending on the flip rate.

---

\*Electronic address: sanoop@physics.iitm.ac.in

†Electronic address: sunil@physics.iitm.ac.in

‡Electronic address: mlaradji@memphis.edu

## I. INTRODUCTION

Biomembranes are non-equilibrium structures due to the non-thermal energy contributions resulting from the activity of a wide variety of vicinal proteins. While the phase behavior and morphology of lipid bilayer membranes have been the subject of extensive amount of studies [1], most of these studies have been on the equilibrium properties of the membranes. This has changed during the last decade or so with investigations of the effects, that active protein pumps have, on the undulations of lipid membranes, their morphology and the normalization of their mechanical constants [2, 3, 4, 5, 6, 7, 8]. Of particular importance is another class of membrane-bound proteins, that actively translocates phospholipids from one leaflet of a biomembrane to the other [9, 10, 11]. The effects of these phospholipid translocators, on the mechanics and morphology of lipid membranes, has not received much attention. In this article, we present a study of self-assembled lipid bilayers in the presence of active lipid translocation, using dissipative particle dynamics simulations.

Lipid synthesis in eukaryotic cells takes place almost exclusively on the cytosolic leaflet of the endoplasmic reticulum (ER), which leads to an asymmetry in the lipid composition across the bilayer. In order to maintain a symmetric lipid density across the ER bilayer, nearly half of the newly synthesized lipids are rapidly translocated to the other leaflet [11]. In contrast, the plasma membrane is marked by an acute asymmetry in the lipid composition. While phosphatidylcholine and sphingomyelin are predominantly present in the exoplasmic leaflet, phosphatidylserine and phosphatidylethanolamine are mainly found in the cytosolic leaflet [12]. Maintenance of the symmetric lipid distribution in ER or the asymmetric lipid distribution in the plasma membrane *cannot* be mediated by thermally induced lipid movements (also termed passive flip-flops) alone. Indeed, passive flip-flops of phospholipids are energetically unfavorable due to the large energy barrier, 20-50 kcal/mol, associated with the translocation of the polar head group through the low dielectric permittivity hydrocarbon core of the bilayer. Consequently, the rate of passive flip-flops of phospholipids is extremely small, of the order of  $10^{-5}\text{s}^{-1}$  [13, 14], i.e. on average, a single lipid experiences a thermally induced flip-flop every 24 hours. The lipid distribution across the bilayer is therefore actively maintained by a class of membrane-bound proteins known as phospholipid translocators [12]. These include the adenosine triphosphate-dependent flippases and floppases, and the energy-independent scramblases [9, 10, 11].

Given the difficulties in purifying membrane-bound proteins, most of lipid translocators have not been identified. Moreover, the mechanism(s) of active flip-flop, mediated by phospholipid translocators, remain elusive. Few models have been proposed as mechanisms for active phospholipid translocations [15, 16]. In particular, Pomorski and Menon [11] recently proposed a mechanism similar to that of swiping a magnetic card through a card reader. In this model, the hydrophobic head group of the flipped/flopped lipid (magnetic strip of the card) is shielded from the hydrophobic environment of the bilayer, thereby facilitating its translocation across the bilayer. Recently, Sens [17] investigated theoretically the conformational response of an infinitely large membrane to a localized disturbance in the form of a localized transbilayer asymmetry in the lipid density. There, he found that this asymmetry may transiently lead to the formation of a bud-like invagination followed by its relaxation.

To our knowledge, the presented work is the first simulation study of the effect of active flip-flop on the mechanical and morphological properties of lipid membranes.

We performed extensive simulations based on dissipative particle dynamics of a lipid bilayer model used previously by us [18, 19, 20] and other groups [21, 22]. In the present study the lipids are translocated across the bilayer using a model reminiscent of the magnetic swipe card mentioned above [11].

## II. BILAYER MODEL

In the dissipative particle dynamics (DPD) model, for a self-assembled lipid bilayer in an explicit solvent used here, a lipid molecule is modeled as a flexible amphiphilic chain of beads consisting of one “head” ( $H$ ) bead attached to three “tail” ( $T$ ) beads via Hookean spring bonds. The solvent is modeled as single beads ( $W$ ). All particles have the same mass  $m$ . In this model, interactions between any two non-bonded particles, within a range  $r_0$ , are soft and repulsive.

The forces acting on particles are grouped into three categories: (i) conservative forces, (ii) dissipative forces, and (iii) random forces. The conservative force between any two particles is

$$\mathbf{F}_{ij}^{(C_1)} = \alpha_{ij}\omega(r_{ij})\hat{\mathbf{r}}_{ij}, \quad (1)$$

where  $\alpha_{ij}$  is the interaction strength between particles  $i$  and  $j$ , at respective positions  $\mathbf{r}_i$  and  $\mathbf{r}_j$ ,  $\mathbf{r}_{ij} = \mathbf{r}_i - \mathbf{r}_j$ , and  $\hat{\mathbf{r}}_{ij} = r_{ij}/|\mathbf{r}_{ij}|$ . Bonded particles belonging to a lipid also experience a

conservative Hookean force given by

$$\mathbf{F}_{i,i+1}^{(C_2)} = -k(1 - r_{i,i+1}/b)\hat{\mathbf{r}}_{i,i+1}, \quad (2)$$

where  $k$  is the spring constant and  $b$  is the preferred bond length. The dissipative force between particles  $i$  and  $j$  is given by

$$\mathbf{F}_{ij}^{(D)} = -\Gamma_{ij}\omega^2(r_{ij})(\hat{\mathbf{r}}_{ij} \cdot \mathbf{v}_{ij})\hat{\mathbf{r}}_{ij}, \quad (3)$$

where  $\Gamma_{ij}$  is the dissipative strength for the pair  $(i, j)$ , and  $\mathbf{v}_{ij} = \mathbf{v}_i - \mathbf{v}_j$  is their relative velocity. The random force between  $i$  and  $j$  is given by

$$\mathbf{F}_{ij}^{(R)} = \sigma_{ij}(\Delta t)^{-1/2}\omega(r_{ij})\zeta_{ij}\hat{\mathbf{r}}_{ij}, \quad (4)$$

where  $\sigma_{ij}$  is the amplitude of the random noise for the pair  $(i, j)$ , and  $\zeta_{ij}$  is a random variable with zero mean and unit variance which is uncorrelated for different pairs of particles and different time steps. Together, the dissipative and random forces act as a thermostat provided the fluctuation-dissipation theorem is satisfied. This yields to the following relation between  $\Gamma_{ij}$  and  $\sigma_{ij}$ ,

$$\sigma_{ij}^2 = 2\Gamma_{ij}k_{\text{B}}T, \quad (5)$$

where  $k_{\text{B}}$  is Boltzmann's constant and  $T$  is the thermostat temperature. In Eqs. (1), (3) and (4), the weight factor,  $\omega(r)$ , is chosen as

$$\omega(r) = \begin{cases} 1 - r/r_0 & \text{for } r \leq r_0 \\ 0 & \text{for } r > r_0, \end{cases} \quad (6)$$

where  $r_0$  is the interactions cutoff. The particles trajectories are obtained by solving Hamilton's equations using the velocity-Verlet integrator [23]. In the simulation,  $r_0$  and  $m$  set the scales for length and mass, respectively.  $k_{\text{B}}T$  sets the energy scale. The time scale is given by  $\tau = (mr_0^2/k_{\text{B}}T)^{1/2}$ . The numerical value of the amplitude of the random force is considered to be the same for all pairs and is given by  $\sigma_{ij} = \sigma = 3.0(k_{\text{B}}^3T^3m/r_0^2)^{1/4}$ , and the fluid density  $\rho = 3.0r_0^{-3}$ . The amplitudes of the conservative force are chosen to be  $\alpha_{HH} = \alpha_{TT} = \alpha_{WW} = \alpha_{WH} = 25k_{\text{B}}T/r_0$  and  $\alpha_{WT} = \alpha_{HT} = 200k_{\text{B}}T/r_0$ . In Eq. (2), the spring constant  $k = 100k_{\text{B}}T$  and  $b = 0.45r_0$ . The time step is chosen to be  $\Delta t = 0.01\tau$ . The flat bilayer is initially constructed parallel to the  $xy$  - plane and placed in the middle of the simulation box. It is then allowed to equilibrate until its normal fluctuations

attain saturation. The total number of lipids used is 16,000 in a simulation box with size  $L \times L \times L_z = (86 \times 86 \times 40)r_0^3$  for the case of symmetric flip-flops and  $(80 \times 80 \times 46)r_0^3$  for the case of asymmetric flip-flops. The system was subject to periodic boundary conditions in all three directions.

### III. FLIP-FLOP SCHEME

We use the following two-step scheme for “flippase” action: (i) formation of a complex and (ii) translocation of a lipid from one leaflet to another. A lipid to be flipped is randomly selected from one of the two leaflets (refer to Figure 1, for a schematic representation of the lipid to be flipped and the surrounding lipid molecules). Around this selected lipid a fictitious cylinder is drawn which spans both leaflets of the bilayer. A flippase complex is then defined as the set of all lipids inside this fictitious cylinder. The next step involves the action of a time-dependent flipping force,  $\mathbf{F}^a(t) = F_z^a(t)\hat{z}$ , on the head bead of the selected lipid, so as to translocate it to the opposite leaflet. This force,  $F_z^a(t)$ , acts in the direction normal to the plane of the bilayer, and its magnitude is given by  $F_z^a(t) = G\Delta z(t)$ , where  $\Delta z(t)$  is the distance between the head bead of the lipid being translocated and the average  $z$ -position of all the lipids, in the complex, in the opposite leaflet. This means that during the translocation process, the amplitude of the flippase force decreases continuously with time. In order to conserve momentum within the fictitious cylinder, a force  $-\mathbf{F}^a(t)/(N_c - 1)$ , where  $N_c$  is the number of lipid molecules in the fictitious complex, is concurrently applied onto the head beads of all other lipids within the flippase complex. During the translocation process of the selected lipid, the head-tail repulsion of the selected lipid, with the other surrounding lipids in the membrane, is “screened” by temporarily choosing its amplitude  $\alpha_{HT} = \alpha_{TT}$ . This algorithm is therefore in-line with the recent swipe card model [11].

In Figure 2 the magnitude of the applied force,  $F_z^a$ , normalized by  $G$ , is shown as a function of time, for the selected lipid as it translocates through the bilayer, mimicking the action of a flippase. This figure depicts that the translocation time scale decreases as the amplitude,  $G$ , of the driving force is increased. In the remaining of the article, all results discussed are based on the case of  $G = 10k_B T/r_0^2$ , for which the typical time taken for flipping a lipid from one layer is about  $\tau$ . During each time step, a number of lipids are selected at random. Flips are attempted with a probability,  $P_{\text{flip}}$ , if the selected lipid is not

already part of an active flipping complex. The success *flip rate* is measured by counting the number of lipids that reach the opposite leaflet in every time step. The flip and flop probabilities are respectively given by,

$$P_{\text{flip}} = \frac{1}{1 + \exp[-A(N_u - N_d - C)]}, \quad (7)$$

and

$$P_{\text{flop}} = \frac{1}{1 + \exp[-A(N_d - N_u + C)]}, \quad (8)$$

where  $N_u$  and  $N_d$  are the numbers of lipid particles in the upper and lower leaflets, respectively. In Eq. (8),  $C$  controls the steady state number difference,  $\Delta N = N_u - N_d$ , and  $A$  is constant which fixes the width of the distribution of  $\Delta N$ . Having developed an active translocation algorithm, we now focus on the effect that active flip-flop has on flat membranes. We consider both cases of symmetric flip-flop,  $C = 0$ , and asymmetric flip-flop,  $C \neq 0$ .

#### IV. SYMMETRIC FLIP-FLOP

Active flip-flop is labeled symmetric, if on average, the number of up-down translocations (flips) is equal to the number of down-up translocations (flops). At the beginning of the simulations, we start with a flat bilayer with exactly the same number of lipids in the two leaflets. We note that the rate of thermally induced flip-flops in this model is practically zero, in accord with experiments. Using the Irving-Kirkwood formalism [24], we calculated the lateral and normal components of the pressure tensor along the  $z$ -axis, and averaged over the  $xy$ -plane [25, 26]. The tension of the membrane and its bending modulus are extracted from the structure factor of the out-of-plane fluctuations of the membrane height [19].

##### A. Membrane Tension and Bending Rigidity

The average orientation of the layer normal is taken to be along the  $z$ -axis. The steady-state profiles of the normal pressure  $P_N(z)$  and the lateral pressure  $P_L(z)$  along the bilayer normal are calculated from the pressure tensor using the Irving-Kirkwood formalism [24]. In Figure 3, the normal and lateral pressure vs.  $z$  of equilibrium membranes are compared with that of membranes active symmetric flip-flop. The rate of flipping is 10 flips/ $\Delta t$  over

a membrane with projected area  $86r_0 \times 86r_0$ . Although the details of the lateral pressure profile is dependent on the model used for the lipids, one observes that the flip-flop activity increases the lateral pressure in the two leaflets while the normal pressure is only weakly affected. As a result, active flip-flop reduces the effective tension on the membrane.

By defining a height field  $h(x, y)$ , which represents the position along the  $z$ -axis of the bilayer mid-plane at a point  $(x, y)$ , and its Fourier transform  $\tilde{h}(\mathbf{q})$  where  $\mathbf{q} = (q_x, q_y)$ , we calculate the circularly averaged structure factor  $S(q) = \langle |\tilde{h}(\mathbf{q})|^2 \rangle / L^2$ , where  $q = (q_x^2 + q_y^2)^{1/2}$ . The long wavelength deformations of a lipid membrane from its mean planar conformation are well described by the Helfrich Hamiltonian [27],  $\mathcal{H}[h(x, y)] = \int dxdy \left[ \frac{\gamma}{2} (\nabla h)^2 + \frac{\kappa}{2} (\nabla^2 h)^2 \right]$ , where  $\gamma$  is the membrane surface tension and  $\kappa$  is its bending modulus. The equipartition theorem of this model yields a structure factor,

$$S(q) = \frac{k_B T}{\gamma q^2 + \kappa q^4}. \quad (9)$$

Hence, by plotting  $k_B T / q^2 S(q)$  as a function of  $q^2$ , one extracts the tension on the membrane,  $\gamma$ , from the intercept with the vertical axis and the bending modulus,  $\kappa$ , from the slope at small wavevectors. This is shown in Figure 4 for the cases of equilibrium and steady state flip-flop with varying flip-flop rates. Figure 4 shows that as the rate of flip-flop is increased, the intercept of  $k_B T / q^2 S(q)$  is shifted to lower values, implying a reduction in the tension of the membrane. This is in line with the results from the lateral and normal pressure shown in Figure 3. However, Figure 4 shows that the slope of  $k_B T / q^2 S(q)$  is independent of the flip-flop rate, implying that for the flip rates considered in our simulation, there does not seem to be any significant effect on the membrane bending modulus due to active flip-flop.

We thus conclude that symmetric active flip-flops leads to an increase in the fluctuations of the membrane, which manifests itself in a decrease of the surface tension of the membrane.

## V. ASYMMETRIC FLIP-FLOP

We now consider the effect of asymmetric flip-flop. In particular, we focus on the case where only lipids from the bottom leaflet are actively flipped to the upper leaflet. This is implemented by assigning a non-zero value for the constant  $C$  in the expression for the probability  $P_{\text{flip}}$  in Eq. (8). The value of  $C$  is kept large, equal to  $10^4$ , such that the rate of accepted flips can be taken as a constant during simulation time. Flipping is restricted to a

small square area ( $l \times l$ ), termed the active region, in the central region of the membrane. This mimics the effect of flips due to localized flippases in a small region of a biomembrane. The effect of asymmetric flipping is then investigated as a function of  $l$  and the total number of flips per unit time ( $\nu$ ).  $l$  is varied between  $10r_0$  to  $50r_0$  and the flip rate is varied from  $\nu = 0.9 \tau^{-1}$  to  $\nu = 20 \tau^{-1}$ .

Asymmetric flip induces a finite difference in the lipid number densities,  $\Delta s = s_u - s_d$ , where  $s_u$  and  $s_d$  are the lipid number densities per unit of area, of the upper and lower leaflets, respectively. Furthermore,  $\Delta s$  increases with time as active flip proceeds. Therefore, asymmetric flip is characterized by an absence of steady state, and if maintained, leads to an instability of the membrane, in contrast to the case of symmetric active flip-flop. We found that asymmetric active flipping lead to the formation of two major transient morphologies corresponding to either buds or blisters, depending on size of the flip area and the flip rate.

When the flip rate is low,  $\nu < 2 \tau^{-1}$ , we found that buds form. This is shown in Figure 5. In this case, a full bud is formed after about  $800\tau$ . Once formed, the bud remains stable even after the flipping is stopped. This is due to the fact that passive flips are practically absent and in-plane lipid diffusion does not homogenize the density in the time scale of the simulation.

When lipids are flipped at a relatively high rate, we observed the formation of blister structures in the active region. In the case with flipping rate  $\nu = 2.5\tau^{-1}$ , it takes about  $300\tau$  for a blister to form. In Figure 6, we depict snapshots showing the main stages of blister formation at this flip rate. The relatively high active flip rate and slow diffusion of the lipids results in high excess of lipids in the upper leaflet. This leads to the detachment of the upper leaflet from the lower leaflet, resulting in a protrusion that is reminiscent of a cylindrical micelle connected to the membrane. This is depicted in Figure 6(a). The cylindrical micelle then grows into a sheet-like structure still connected to the membrane, as shown in Figure 6(b). If the process of active flipping is further continued, we found that the membrane becomes unstable. To avoid a destabilization of the membrane, we consider only the cases, where active flipping is stopped once the sheet-like structure (Figure 6(b)) is formed. The relaxation of the blister depends on the stage at which active flipping is halted. If active flipping is stopped during the early stage of blister formation, shown in Figure 6(a), the blister relaxes back into the membrane. At late stages, when the sheet is well formed (see Figure 6(b)), in order to reduce the high edge energy, the blister curves



forming a hook-like structure shown in Figure 6(c). Eventually, the sheet closes on to the membrane, forming a hemifusion state, reminiscent of that observed during the intermediate stages of vesicles fusion [28]. This is elucidated in the series of snap shots shown in Figure 6(b-e). Eventually, the diaphragm in the hemifusion state ruptures into a pore as shown in Figure 6(f). If active flip is stopped at an intermediate stage between those shown in Figure 6(a) and (b), the blister relaxation is arrested at the hemifusion state shown in Figure 7(b).

## VI. CONCLUSION

The thickness of the bilayer obtained in the simulations is  $4r_0$ . Comparing this with the thickness of lipid bilayers, 5 nm, we obtain  $r_0 \approx 1.25\text{nm}$ . In phospholipid bilayers in the fluid phase, the diffusion coefficient of a lipid is typically  $D \sim 10^{-12}\text{m}^2/\text{s}$ , refer [12]. Comparing this with the diffusion coefficient for lipids obtained in the current simulations, one can estimate the DPD time unit,  $\tau \approx 0.2\mu\text{s}$ . For the case of  $G = 5$ , we then find that the average duration of a single flip is about  $2\mu\text{s}$ . Considering that the time scale for typical protein conformation change ranges from milliseconds to seconds, to make contact with real systems, one has to use smaller values of  $G$ . However, for practical reasons we use  $G = 10$ . The typical simulation run in the present work is about  $200\mu\text{s}$  corresponding to a diffusion length of approximately  $15\text{nm}$ . This implies that the flip-flop time scale in the current simulation is faster than the time scale associated with in-plane diffusion of lipids. We therefore conclude that the budding event seen in the current simulation is a non-equilibrium process. In the case of an infinite membrane this bud will disappear on time scales larger than diffusion time. However in finite systems the resulting area difference of the two leaflets leads to buds that are stable within the time scale set by passive flip-flop rates.

The initial tension on the membrane also plays a role in determining the critical flip rate for bud and blister formation. In the case of membranes with fixed projected area, asymmetric flipping from the bottom leaflet to the upper leaflet leads to an asymmetry in the area per lipid in the two leaflets of the membrane. This in turn leads to an increase in the lateral tension of the bottom leaflet while that of the upper leaflet decreases. In order to equalize the area per lipid in the two leaflets, the membrane buckles, which will further

increase the tension in both the leaves. Beyond a critical tension, the bottom leaflet will either rupture or decouple from the upper leaflet resulting in a blister. This also means that the flip rate at which blisters start to form should decrease with increasing tension of the initial equilibrated membrane. We confirm this in our simulations.

In conclusion, we have presented a DPD model to study active flipping and its effects on a fluid bilayer membrane. We find that symmetric flip-flop results in a reduction in the tension of the membrane without much effect on its bending modulus. Asymmetric flip-flop results in non-equilibrium structures depending on the lipid flip rate. Slow flip rates involves membrane curvature and bud formation, whereas fast flip rates induces blister formation.

### Acknowledgements

PBSK acknowledges DST India for financial support. ML acknowledges the financial support through a grant from the Research Corporation (Award No. CC6689). MEMPHYS is supported by the Danish National Research Foundation.

- 
- [1] O. G. Mouritsen, *Life - As a Matter of Fat* (Springer-Verlag, Berlin, 2005).
  - [2] J. B. Manneville, P. Bassereau, D. Levy and J. Prost, Phys. Rev. Lett., **82**, 4356 (1999).
  - [3] S. Ramaswamy, J. Toner, and J. Prost, Phys. Rev. Lett., **84**, 3594 (2000).
  - [4] N. S. Gov, Phys. Rev. Lett., **93**, 268104 (2004).
  - [5] N. S. Gov and S. A. Safran, Biophys. J., **88**, 1859 (2000).
  - [6] M. A. Lomholt, Phys. Rev. E., **73**, 061913 (2006).
  - [7] A. Giahhi, M. E. A. Faris, P. Bassereau, and T. Salditt, Eur. Phys. J. E., **23**, 031925 (2007).
  - [8] R. Shlomovitz and N. S. Gov, Phys. Rev. Lett., **98**, 168103 (2007).
  - [9] D. L. Daleke, J. Lipid Res., **44**, 233 (2003).
  - [10] P. F. Devaux, I. Lopez-Montero, and S. Bryde, Chem. Phys. Lipids, **141**, 119 (2006).
  - [11] T. Pomorski and A. K. Menon, Cell. Mol. Life Sci., **63**, 2908 (2006)
  - [12] B. Alberts, D. Bray, J. Lewis, M. Raff, K. Roberts, and J. D. Watson, *Molecular Biology of the Cell* (Garland, New York, 1994).
  - [13] M. S. C. Abreu, M. J. Moreno, and W. L. C. Vaz, Biophys. J., **87**, 353 (2004).

- [14] J. Liu and J. C. Conboy, Biophys. J., **89**, 2522 (2005).
- [15] K. E. Langley and E. P. Kennedy, Pro. Nat. Acad. Sci. USA, **76**, 6245 (1979).
- [16] M. A. Kol, A. I. de Kroon, J. A. Killian, and B. de Kruijff, Biochem., **43**, 2673 (2004).
- [17] P. Sens, Phys. Rev. Lett., **93**, 108103 (2004).
- [18] M. Laradji and P. B. S. Kumar, Phys. Rev. Lett., **93**, 198105 (2004).
- [19] M. Laradji and P. B. S. Kumar, J. Chem. Phys., **123**, 224902 (2005).
- [20] M. Laradji and P. B. S. Kumar, Phys. Rev. E., **73**, 040901 (2006).
- [21] S. Yamamoto, Y. Maruyama, and S. -A. Hyodo, J. Chem.Phys., **116**, 5842 (2002).
- [22] J. Shillcock and R. Lipowsky, J. Chem. Phys., **117**, 5048 (2002).
- [23] G. Besold, I. Vattulainen, M. Karttunen, and J. M. Polson, Phys. Rev. E, **62**, R7611 (2000).
- [24] J. Irving and J. Kirkwood, J. Chem. Phys., **18**, 817 (1950).
- [25] P. Schofield and J. R. Henderson, Proc. R. Soc. Lon. A, **379**, 231 (1982).
- [26] R. Goetz and R. Lipowsky, J. Chem. Phys., **108**, 7397 (1998).
- [27] W. Helfrich, Z. Naturforsch., **28c**, 693 (1973).
- [28] J. Shillcock and R. Lipowsky, Nat. Mater., **4**, 225 (2005).

## List of Figures

- 1 Flippase complex corresponding to the fictitious cylinder containing the lipid to be flipped. The lipid to be flipped is shown explicitly. However, only head beads of the other lipids in the flippase complex are shown. . . . . 14
- 2 Normalized amplitude of the translocation force,  $F_z^a(t)/G$ , vs. time for four values of the force magnitude,  $G$ . The data has been averaged over all translocated lipids and over time during steady state. . . . . 15
- 3 Normal pressure  $P_N$  and lateral pressure  $P_L$  as a function of  $z$  (both equilibrium and with an attempted flip rate of 10 flips per  $\Delta t$ ) for a system with  $L = 86r_0$  and  $k_B T = 1.0$ . . . . . 16
- 4 Structure factor vs.  $q^2$  for different values of attempted flip rates. Different symbols correspond to the cases of equilibrium ( $\square$ ), 1 flip/ $\Delta t$  ( $\blacksquare$ ), 2 flips/ $\Delta t$  ( $\circ$ ), 5 flips/ $\Delta t$  ( $\bullet$ ), and 10 flips/ $\Delta t$  ( $\triangle$ ). The simulations are performed on a system containing 16000 lipids with  $L = 86r_0$  and  $k_B T = 1.0$ . . . . . 17

5	Bud Formation (only a small section of the membrane, with a cut through the budding region, is shown). a) Initial bending of both the leaflets and b) neck formation which eventually leads to a bud. The flip rate and size of the active region are $\nu = 0.9\tau^{-1}$ and $l = 10$ respectively. . . . .	18
6	Blister Formation (only a small section of the membrane, with a cut through the blister, is shown). a) Initial protrusion b) sheet formation c-e) fusion of sheet with membrane and f) pore formation. Note that the edge of the blister, clearly visible in in (b), moves towards the cut plane in (b) to (e). The flip rate and size of the active region are $\nu = 2.5\tau^{-1}$ and $l = 30$ respectively. . . .	19
7	In its early stage blisters can also relax by folding into itself, forming a bulb-like structure. . . . .	20

## Figures

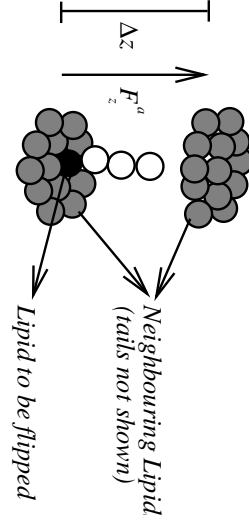


FIG. 1: Flippase complex corresponding to the fictitious cylinder containing the lipid to be flipped. The lipid to be flipped is shown explicitly. However, only head beads of the other lipids in the flippase complex are shown.

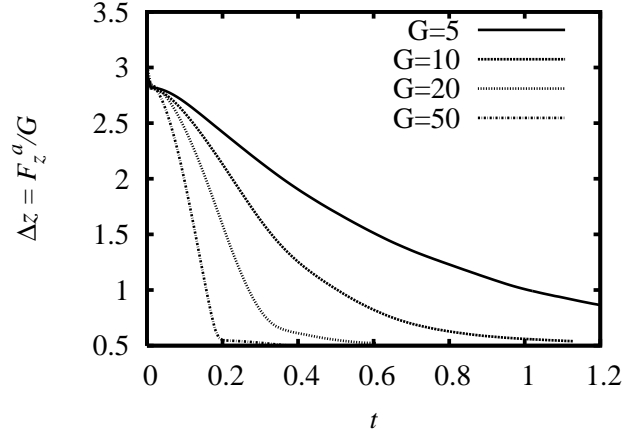


FIG. 2: Normalized amplitude of the translocation force,  $F_z^a(t)/G$ , vs. time for four values of the force magnitude,  $G$ . The data has been averaged over all translocated lipids and over time during steady state.

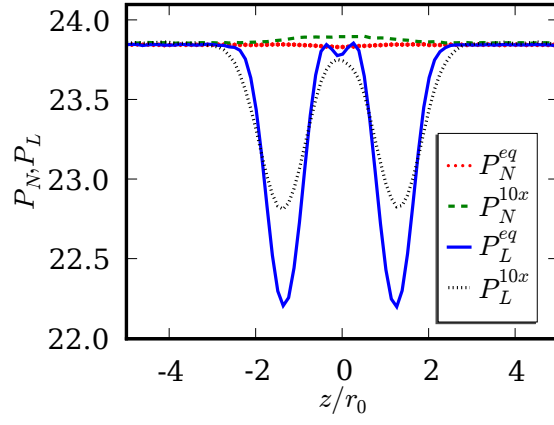


FIG. 3: Normal pressure  $P_N$  and lateral pressure  $P_L$  as a function of  $z$  (both equilibrium and with an attempted flip rate of 10 flips per  $\Delta t$ ) for a system with  $L = 86r_0$  and  $k_B T = 1.0$ .



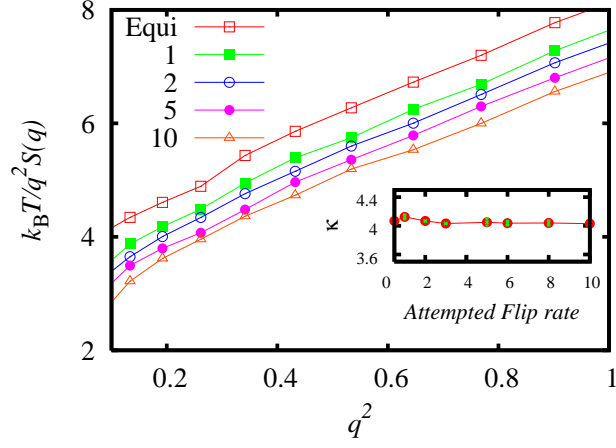


FIG. 4: Structure factor vs.  $q^2$  for different values of attempted flip rates. Different symbols correspond to the cases of equilibrium ( $\square$ ), 1 flip/ $\Delta t$  ( $\blacksquare$ ), 2 flips/ $\Delta t$  ( $\circ$ ), 5 flips/ $\Delta t$  ( $\bullet$ ), and 10 flips/ $\Delta t$  ( $\triangle$ ). The simulations are performed on a system containing 16000 lipids with  $L = 86r_0$  and  $k_B T = 1.0$ .

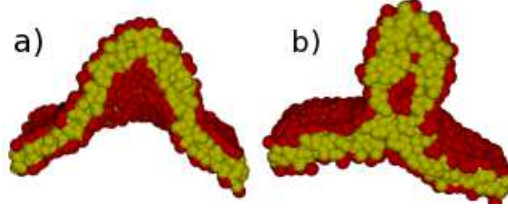


FIG. 5: Bud Formation (only a small section of the membrane, with a cut through the budding region, is shown). a) Initial bending of both the leaflets and b) neck formation which eventually leads to a bud. The flip rate and size of the active region are  $\nu = 0.9\tau^{-1}$  and  $l = 10$  respectively.

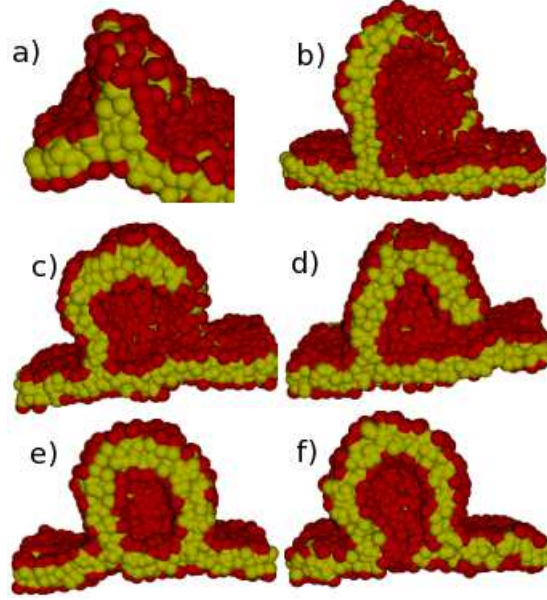


FIG. 6: Blister Formation (only a small section of the membrane, with a cut through the blister, is shown). a) Initial protrusion b) sheet formation c-e) fusion of sheet with membrane and f) pore formation. Note that the edge of the blister, clearly visible in in (b), moves towards the cut plane in (b) to (e). The flip rate and size of the active region are  $\nu = 2.5\tau^{-1}$  and  $l = 30$  respectively.

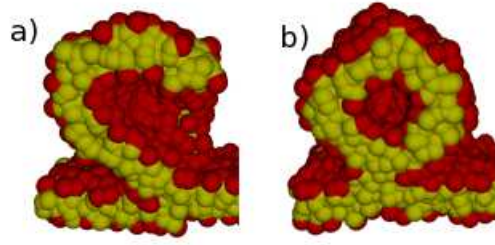


FIG. 7: In its early stage blisters can also relax by folding into itself, forming a bulb-like structure.